14.3 ENHANCEMENT OF POLAR WRF ATMOSPHERIC AND SURFACE PROCESSES: A CONTRIBUTION TO ARCTIC SYSTEM REANALYSIS AND PUBLIC AWARENESS*

Aaron B. Wilson[1,2], David. H. Bromwich[1,2], Keith M. Hines[1], and Carol E. Landis[3]

[1]Polar Meteorology Group, Byrd Polar Research Center, The Ohio State University Columbus, Ohio
[2]Atmospheric Sciences Program, Department of Geography, The Ohio State University Columbus, Ohio
[3]Education Outreach Specialist, Byrd Polar Research Center, The Ohio State University Columbus, Ohio

1. INTRODUCTION

Climate change in the Arctic has become a key topic among climate researchers in recent years. Stimulated by the record summer sea ice minima in 2007 and 2008 (NSIDC 2007) and the growing scientific interest in the region (Kerr 2009; Lindsay et al. 2009), scientists are accelerating efforts to evaluate the reasons for and the effects of this changing polar landscape. Of concern is the question of Arctic warming and sea ice retreat and whether the changes being seen are a signal of global warming.

Sea ice is an important factor in the global climate system, covering 5%-8% of the global oceans (Comiso et al. 2003). Responsible for the regulation of heat exchange between the ocean and the atmosphere, sea ice and snow cover on sea ice effectively insulate one from the other (Powell et al. 2005). Likewise, with their high albedo (0.65-0.90), sea ice and snow cover are extremely important for the reflectance of the sun's energy back into space, controlling the earth's temperature. Therefore, it is paramount that researchers using state-of-the-art models, such as the Weather Research and Forecasting Model (WRF), understand the role sea ice and snow cover albedo play throughout the Arctic Basin. This understanding will allow researchers to create models with configurations most accurately describing true Arctic conditions. To this end, consideration of snow cover albedo, sea ice concentration throughout the Arctic sea ice zone, sea ice thickness, seasonal progression of sea ice albedo and seasonal coverage of melt ponds must be accounted for within any model of the Arctic region. This will ensure proper heat and momentum exchanges between the ocean and atmosphere, leading to model results that are reflective of the polar environment.

Previous modeling of the Arctic environment includes the development and testing of a polar optimized version of WRF (PWRF). The development and testing of this model has been conducted by the Polar Meteorology Group (PMG) at The Ohio State University, similar to the development of Polar MM5 made by the PMG using the fifth generation Pennsylvania State University/National Center for Atmospheric Research Mesoscale Model (Dudhia 1993). Changes to the surface energy balance equation within the Noah land scheme and treatment of snowpack are made while modeling ice sheet surface conditions on a Greenland domain (Hines and Bromwich 2008). Likewise, PWRF is evaluated over the Arctic Ocean (Bromwich et al. 2009a) by comparing model results with measurements made during the Surface Heat Budget of the Arctic Ocean (SHEBA) from 1997-1998 (Perovich et al. 1999; Uttal el al. 2002). Substantial changes include the treatment of sea ice fraction and seasonal variation of Arctic Ocean sea ice albedo based on a freeze-thaw cycle (Perovich et al 2007). Finally, evaluation and development of PWRF over Arctic land surface is currently ongoing (Hines et al. 2009), and further development of PWRF is planned.

* *Corresponding author address:* Aaron B. Wilson,
Polar Meteorology Group, Byrd Polar Research Center,
The Ohio State University, 1090 Carmack Rd.
Columbus, Ohio 43210-1002; email: wilson.1010@osu.edu

In continuing the evaluation of PWRF throughout the Arctic, simulations of Arctic conditions with WRF and PWRF on the ASR domain are investigated. The goal is to examine key characteristics of weather patterns in the Arctic, including the Arctic river basins and surrounding lower latitudes for the entire year of 2007. In addition to using previous PWRF improvements to the Noah land scheme and fractional sea ice, future improvements to PWRF will include sea ice thickness specified as thick multiyear sea ice or thin seasonal sea ice and allowed to vary for the entire year accordingly. Similarly, seasonal progression of sea ice albedo and treatment of Arctic melt ponds will be addressed to ensure proper albedo over all sea ice surfaces. This analysis and enhanced description of atmospheric and surface processes in WRF will produce a robust model that will be used to simulate Arctic conditions for the Arctic System Reanalysis (ASR; Bromwich et al. 2009b). ASR will provide a synthesis of modeling data, observations, field work, and satellite measurements in order to provide a comprehensive reanalysis of the entire Arctic basin for the period 2000-2010. Furthermore, this newly optimized version of Polar WRF will be used for outreach between scientists at the Byrd Polar Research Center of The Ohio State University and students at the Columbus Zoo and Aquarium through the Polar Frontier Project.

Here, results of simulations for December 2007 are presented as a baseline for future work. Section 2 provides data and methods, including WRF and PWRF configurations. Results comparing 2m temperature, 2m dewpoint temperature, surface pressure, mean sea level pressure, 10m wind speed, and 10m wind components (zonal and meridional) are discussed in section 3. Section 4 is a detailed analysis of model results for Calgary, Alberta Canada highlighting the need for increased horizontal resolution in ASR simulations. Section 5 shows preliminary upper level comparisons, specifically upper level temperature results at 850hPa and 500hPa. Finally, summary and conclusions are drawn in section 6.

2. DATA AND METHODS

2.1 Model Configurations

Several configurations of WRF and PWRF are evaluated for December 2007 over the entire ASR domain (Fig.1). The goal is to capture not only the immediate Arctic environment, but also the entire Arctic river basin drainage area.

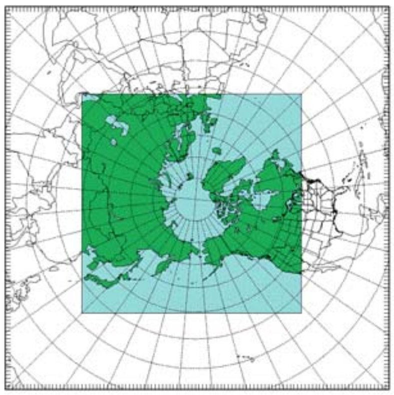

Figure 1. Model domain for all WRF and PWRF configurations. Inner domain has 181 x 181 grid points with 60km resolution.

The 2-way nested domains are centered on the North Pole, with the inner domain extending 10,800km in the east-west and north-south directions with 60km resolution. The lateral boundary conditions are specified by the National Centers for Environmental Prediction (NCEP) Final Analysis data (FNL), a 1° x 1° global grid updated every 6 hours. The simulations are performed in 48 hour increments initialized daily at 0000UTC, with the first 24 hours of model output discarded for model spin-up.

All simulations include 39 vertical terrain-following sigma levels, with the top boundary set high (10hPa) for better treatment of upward propagating gravity waves (Bromwich et el. 2005). Likewise, the Rapid Radiative Transfer Model longwave radiation scheme, Goddard shortwave radiation scheme, Mellor-Yamada-Janjic planetary boundary layer scheme, and the NCEP/NCAR/AFWA unified Noah Land Surface Model with Eta similarity surface layer are employed in all model simulations following the work conducted with earlier versions of Polar WRF (Hines and Bromwich 2008; Bromwich et al. 2009a). Differences among the simulations are reflected in the following choices: cumulus parameterizations (Kain-Fritsch or Grell-Devenyi), lower boundary sea ice (FNL or Bootstrap Sea Ice Concentration from the Defense Meteorological Satellite Program's (DMSP) Special Sensor Microwave/Imager (SSM/I); Comiso 1999), lower boundary sea surface temperatures (FNL Skin Temperature or NCEP 0.5° RTG_SST Analysis; Gemmill et al. 2007), and albedo changes to the Noah LSM. Model is output at 3-hour intervals with a 240 second time step.

2.2 Data

Figures 2a-b shows selected observation sites for comparison with surface and upper level variables. Surface observations of station and mean sea level pressure, 2m temperature, 2m dewpoint, 10m wind, and cloud and precipitation measurements are obtained through the National Climatic Data Center FTP access. Although 78% of model surface elevations are within 200m of NCDC elevations, 2m temperature and 2m dewpoint results from model simulations are adjusted to NCDC station height using the environmental lapse rate of 0.0065 K m^{-1}. Likewise, model surface pressure is corrected hydrostatically to NCDC station elevations for all locations where surface pressure is available (mean sea level pressure compared when surface pressure is unavailable).

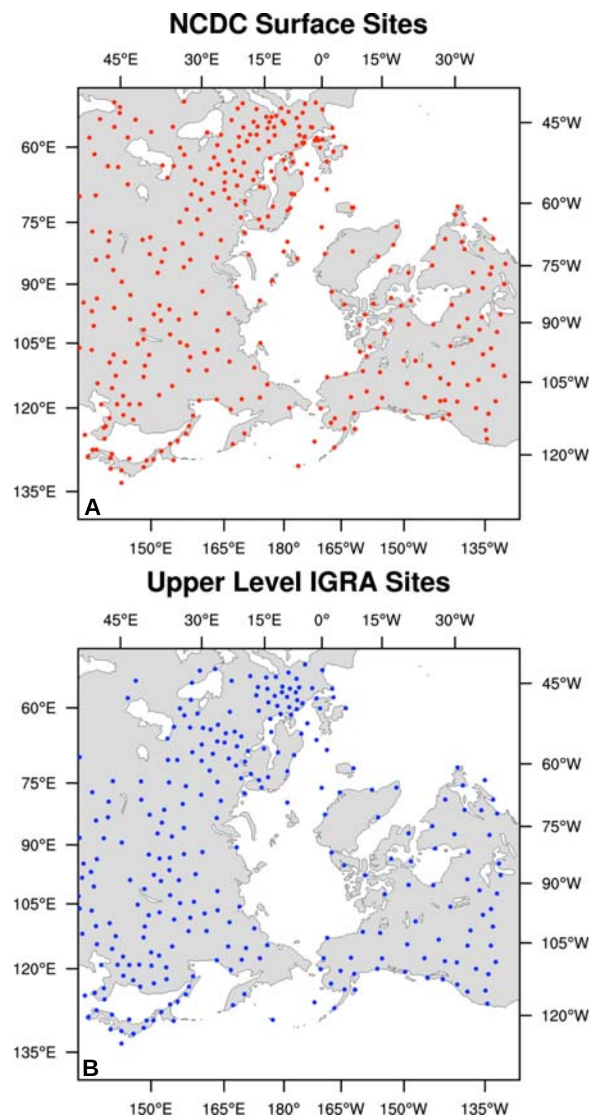

Figure 2. A) Surface observation sites provided by NCDC Climate Data Online. **B)** Upper level observation sites provided by IGRA derived product data set.

MODEL - OBSERVATIONS

2m TEMPERATURE (°C)							
MODEL RUN	**REGION**	**BIAS**	**MAX**	**MIN**	**STD.**	**RMSD**	**CORR.**
STD WRF3.0.1.1(Grell)	Lower	2.09	18.24	-6.40	2.58	4.05	0.79
PWRF3.0.1.1(Grell/Albedo2/SSM/I)	Lower	1.96	17.79	-4.41	2.53	4.00	0.79
STD WRF3.0.1.1(Grell)	Polar	-0.45	5.73	-6.15	2.96	4.33	0.79
PWRF3.0.1.1(Grell/Albedo2/SSM/I)	Polar	0.19	6.21	-3.34	2.56	4.20	0.78
2m DEWPOINT (°C)							
MODEL RUN	**REGION**	**BIAS**	**MAX**	**MIN**	**STD.**	**RMSD**	**CORR.**
STD WRF3.0.1.1(Grell)	Lower	2.51	16.38	-4.73	2.35	4.32	0.80
PWRF3.0.1.1(Grell/Albedo2/SSM/I)	Lower	2.50	16.42	-2.56	2.35	4.31	0.79
STD WRF3.0.1.1(Grell)	Polar	-0.36	5.74	-6.89	3.10	4.62	0.81
PWRF3.0.1.1(Grell/Albedo2/SSM/I)	Polar	0.36	7.09	-4.53	2.82	4.56	0.80
SURFACE PRESSURE (hPa)							
MODEL RUN	**REGION**	**BIAS**	**MAX**	**MIN**	**STD.**	**RMSD**	**CORR.**
STD WRF3.0.1.1(Grell)	Lower	-1.36	9.83	-10.35	2.15	3.56	0.96
PWRF3.0.1.1(Grell/Albedo2/SSM/I)	Lower	-1.34	10.17	-10.26	2.19	3.58	0.96
STD WRF3.0.1.1(Grell)	Polar	-0.54	8.64	-4.48	2.98	3.59	0.97
PWRF3.0.1.1(Grell/Albedo2/SSM/I)	Polar	-0.85	7.81	-4.25	2.84	3.71	0.97
SEA LEVEL PRESSURE (hPa)							
MODEL RUN	**REGION**	**BIAS**	**MAX**	**MIN**	**STD.**	**RMSD**	**CORR.**
STD WRF3.0.1.1(Grell)	Lower	-3.55	1.74	-27.08	3.37	4.95	0.96
PWRF3.0.1.1(Grell/Albedo2/SSM/I)	Lower	-3.54	1.91	-27.01	3.37	4.96	0.96
STD WRF3.0.1.1(Grell)	Polar	-1.65	1.45	-3.20	1.14	3.35	0.97
PWRF3.0.1.1(Grell/Albedo2/SSM/I)	Polar	-1.99	1.13	-3.31	1.09	3.62	0.97
10m WIND SPEED (m/s)							
MODEL RUN	**REGION**	**BIAS**	**MAX**	**MIN**	**STD.**	**RMSD**	**CORR.**
STD WRF3.0.1.1(Grell)	Lower	2.31	7.49	-2.45	1.45	3.44	0.57
PWRF3.0.1.1(Grell/Albedo2/SSM/I)	Lower	2.36	8.66	-2.41	1.47	3.46	0.57
STD WRF3.0.1.1(Grell)	Polar	0.08	3.84	-3.36	2.01	3.42	0.59
PWRF3.0.1.1(Grell/Albedo2/SSM/I)	Polar	0.91	6.43	-2.03	2.06	3.56	0.60
10m ZONAL U-WIND (m/s)							
MODEL RUN	**REGION**	**BIAS**	**MAX**	**MIN**	**STD.**	**RMSD**	**CORR.**
STD WRF3.0.1.1(Grell)	Lower	-0.31	5.33	-7.29	2.06	4.80	0.60
PWRF3.0.1.1(Grell/Albedo2/SSM/I)	Lower	-0.30	6.44	-7.37	2.07	4.80	0.60
STD WRF3.0.1.1(Grell)	Polar	-0.11	4.94	-12.75	3.92	7.80	0.58
PWRF3.0.1.1(Grell/Albedo2/SSM/I)	Polar	-0.22	5.17	-12.18	3.69	7.62	0.58
10m MERIDIONAL V-WIND (m/s)							
MODEL RUN	**REGION**	**BIAS**	**MAX**	**MIN**	**STD.**	**RMSD**	**CORR.**
STD WRF3.0.1.1(Grell)	Lower	0.36	13.24	-8.67	2.58	5.34	0.54
PWRF3.0.1.1(Grell/Albedo2/SSM/I)	Lower	0.34	13.02	-8.63	2.56	5.34	0.54
STD WRF3.0.1.1(Grell)	Polar	0.24	7.15	-5.73	3.68	8.36	0.61
PWRF3.0.1.1(Grell/Albedo2/SSM/I)	Polar	0.34	6.36	-5.38	3.34	8.19	0.60

Table 1. Mean bias, maximum and minimum bias, standard deviation, root mean squared difference, and correlation for Standard and Polar WRF. For each variable, the domain is broken down into poleward of 70°N (Polar=21 stations) and the rest of the domain (Lower=299 stations). Temperature and dewpoint are given in °C, pressure variables in hPa, and wind variables in ms^{-1}.

Upper level comparisons are made with the Integrated Global Radiosonde Archive (IGRA) sounding-derived data set which includes observations for pressure, geopotential height, and temperature (Durre and Yin 2008). Likewise, derived variables including potential temperature, relative humidity, saturation vapor and vapor pressure, and zonal and meridional wind components are available for comparison.

3. SURFACE RESULTS

The analysis of both standard and polar versions of WRF begins with a detailed evaluation of model performance compared to observations (Model – Observations) spread throughout the entire ASR domain. The key difficulty in configuring the model simulations is the expansiveness of the domain itself. Choosing the physical parameterizations that work throughout the domain is a challenge. The ultimate goal is to configure WRF in such a way that one gets reliable performance in the Arctic and the surrounding lower latitudes. This includes accurate representations of surface and upper air processes, as well as proper radiative and moisture fluxes in all areas of the domain. Likewise, a horizontal resolution of 60km and 39 vertical layers are chosen here for all model simulations in order to limit expense of computational resources. One can expect that errors between model simulations and surface observations will occur as a result of the coarse spatial resolution chosen for these simulations.

First, to test the cumulus parameterization, a sensitivity study using Standard WRF shows improvement in switching from the Kain-Fritsch (Kain 2004) to the Grell-Devenyi cumulus scheme (Grell and Devenyi 2002). This may be attributed to the fact that the Grell-Devenyi scheme uses multiple cumulus schemes within each grid box and averages them for better representation of cloud processes, such as detrainment and precipitation.

Similarly, a sensitivity study of snow cover albedo is conducted using PWRF. Snow cover on sea ice changes both the albedo and ocean to atmosphere heat and moisture fluxes (Lindsay and Zhang 2006). Likewise, the amount of radiation reflected to space increases when snow cover is present on land receiving any amount of sunlight. However, with little solar radiation reaching the surface in the Arctic during December, one might expect that a change in the snow cover albedo over the sea ice will have no effect on near surface temperature and dewpoint. On the other hand, changes in the snow cover albedo on land at the lower latitudes would change the amount of solar radiation absorbed. Therefore, one might expect small improvements to temperature and dewpoint at lower latitudes where fresh snow cover albedo would be important in December. For this sensitivity run, the snow cover albedo is changed from 0.70 to 0.80 in the Noah Land Surface Model, and small improvements to model mean 2m temperature, 2m dewpoint temperature, and pressure variable biases are realized. This indicates that although the change in snow cover albedo north of the Arctic Circle in December has no bearing on near surface temperature and dewpoint, the snow cover albedo on land in the surrounding lower latitudes included in the domain is important to overall model performance, and 0.80 is a better value at this time. Additionally, using a polar version of WRF with sea ice concentration from the DMSP SSM/I (Comiso 1999, 2008) makes small improvements to the overall model performance as well, and this configuration is used for further analysis of WRF performance in the Arctic.

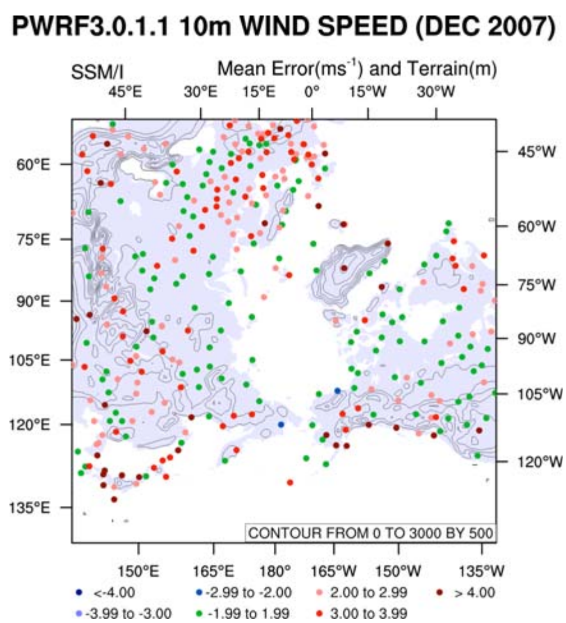

Figure 3. 10m wind speed bias in ms^{-1} for PWRF3.0.1.1. Terrain is contoured 0 to 3000m in steps of 500m.

In order to evaluate further the improvements that Polar WRF provides for Polar Regions, surface observations are divided into two subsets. One subset includes all stations 70°N latitude and northward (Polar) and the other includes the remainder of the stations in the ASR domain (Lower). Statistics are calculated for these subsets and can be found in Table 1.

Mean biases for 2m temperature, 2m dewpoint temperature, surface pressure and mean sea level pressure are good for both standard and polar versions of WRF in the entire domain. Pressure variables show excellent skill throughout the domain and slightly higher correlations for stations included in the Polar subset.

Polar WRF improved mean bias 2m temperature, especially in areas north of 70°N. Both temperature and dewpoint reflect a slight warm bias in the polar version as compared to the cold bias with the standard WRF, a result of mixed ice and open water (Bromwich et al. 2009a).

Equally encouraging is PWRF's ability to maintain good model performance, even in lower latitudes. In fact, PWRF improves 2m temperature, pressure, and 10m zonal and 10m meridional wind bias over standard WRF with no major degradation in the other examined variables.

However, 10m wind speed biases for stations in the Lower subset are high (Fig. 3). Note the larger biases across Europe and Central Asia compared to the smaller biases found at stations along the Arctic Ocean. While Table 1 shows the model's improved performance for stations north of 70°N, wind characteristics are not easily captured by the model. This is a likely result of 60km horizontal resolution and the inability to represent local changes to wind speed and direction, especially near steep topography.

4. CALGARY SITUATION

While evaluating model simulations for various stations within the ASR domain, Calgary, Alberta Canada presents evidence for problems when dealing with coarse horizontal resolution.

Calgary is located just to the east side of the Rocky Mountains (latitude 51.12N, longitude 114.02W, elevation 1084m) in a transition from mountain to plain terrain. Calgary's climate is primarily semi-arid owing largely to the fact that it is on the orographic shadow side of the mountains. Figures 4a-b shows the 2m temperature and 2m dewpoint time series for the month of December 2007. Notice the large deviation between the model and observations for days 3-6. The model reflects a large influx of warmer 2m temperatures along with an increase in 2m dewpoint temperature.

Likewise, looking at the time series of mean sea level pressure for Calgary during the same period shows a distinct drop in the pressure, nearly 20hPa lower in the model (Fig. 5). This suggests that an area of low pressure moving in off the Pacific toward Calgary may have been able to penetrate much farther inland in the model simulation that would have otherwise been restricted by the Rocky Mountains. After analyzing an animation of model mean sea level pressure and temperatures with surface analysis provided by the Hydrological Prediction Center (not shown), indeed the model Pacific low pressure center travels farther inland toward Calgary. It is hypothesized, that an increase in horizontal resolution, like one implemented in the ASR (10-15km) should improve cases where orographic effects play a major role in a location's weather and climate.

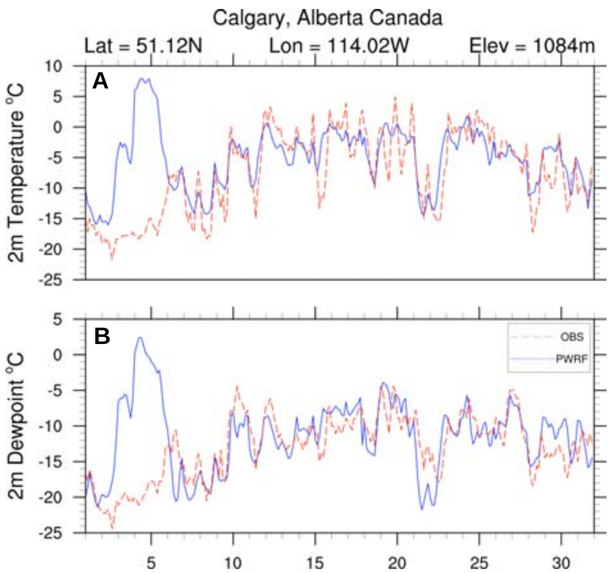

Figure 4. A) 2m temperature time series for Calgary, Alberta Canada for December 2007. **B)** 2m dewpoint temperature time series for Calgary, Alberta Canada for December 2007.

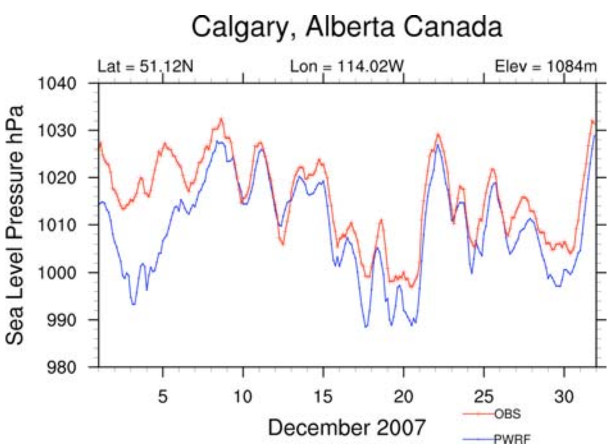

Figure 5. Mean sea level time series for Calgary, Alberta Canada for December 2007.

5. UPPER LEVEL RESULTS

In order to evaluate the model performance of upper level atmospheric processes, model results of vertical temperature profiles, moisture profiles, and wind profiles are compared to observations from the Integrated Global Radiosonde Archive derived data set (described earlier) at 1000hPa, 850hPa, 700hPa, 500hPa, 300hPa, 200hPa, and 100hPa. Figures 6a-b shows 850hPa and 500hPa temperature bias for the entire domain for December 2007 using the PWRF with SSM/I sea ice concentration. For 850hPa, 8 out of 266 upper level station comparisons are discarded from the statistical analysis, lying outside of 3 standard deviations from the mean bias. Similarly, 12 out of 279 stations on the 500hPa level are eliminated. As a result, 231 out of 258 850hPa temperature comparisons have mean biases within ± 2°C; 260 out of 267 stations for

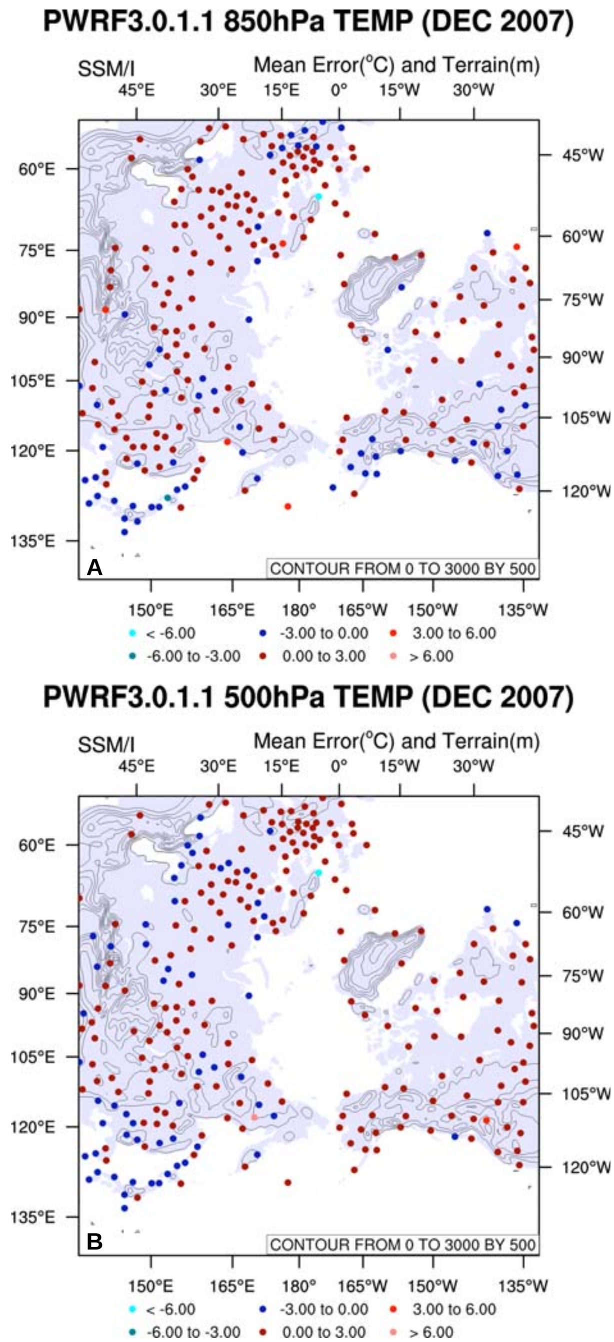

Figure 6. A) 850hPa temperature mean bias for model minus IGRA observations. **B)** 500hPa temperature mean bias model minus observations.

500hPa. Larger errors occur in higher terrain areas in the Alps and throughout Japan. Overall, both 850hPa and 500hPa model results are slightly warmer than observations, 0.54°C and 0.44°C mean error respectively. Likewise, both show good skill of 0.81 and 0.83, capturing two-thirds of the variability. While the results from upper level comparisons are preliminary, they show promise that the PWRF accurately represents upper level temperature profiles. Similar analysis of upper level humidity, geopotential height, and winds is ongoing.

6. CONCLUSIONS

It has been demonstrated that PWRF simulations of the ASR domain have resulted in good performance for most surface variables as well as upper level temperature profiles for varying configurations of PWRF. Simulations have resulted in excellent agreement between model and observations for surface pressure variables. In addition, model results of 2m temperature and 2m dewpoint show good performance throughout the domain, except for coastlines and regions with complex topography. One area of needed improvement is simulated 10m wind characteristics, with likely improvements to occur with increased horizontal resolution. Some surface stations are suboptimal, presenting a difficult challenge in modeling local wind effects. Increased horizontal resolution will allow for local variability and likely improved agreement between model and observations, as well as a better representation of the effects mountains impose on local environments. Likewise, anticipated improvements to Polar WRF (sea ice thickness and seasonal progression of albedo) will provide a more accurate depiction of heat and momentum exchanges between the ocean and the atmosphere in Polar Regions. Furthermore, upper level temperature profiles throughout the column show good agreement between model and observations (most model mean temperatures within ± 2°C). This demonstrates PWRF's ability to accurately describe the temperature profile throughout the troposphere.

Despite the success shown by these preliminary results, analysis of additional variables such as precipitation, clouds, upper level moisture and heights, as well as radiative variables are ongoing. Simulations for December 2007 will serve as a basis for simulations throughout 2007. The ultimate goal is to produce a robust and accurate model representation of the Arctic environment. Overall, PWRF has demonstrated its ability for use in Arctic simulations, and with the expected improvement to sea ice treatment, will be beneficial for use in ASR. Additionally, PWRF will be implemented in short term weather forecasts of the Arctic. This will serve as both learning and teaching tool in outreach programs, such as the Polar Frontier Project.

7. ACKNOWLEDGMENTS

This research is funded by The Ohio State University Engagement in Education Committee Polar Frontier Project with the Columbus Zoo and Aquarium, NSF IPY Grant 0733023, and DOE Award GRT00008066. The authors thank Dr. Francis Otieno of Byrd Polar Research Center for discussion on model configuration, results, and display.

8. REFERENCES

Bromwich, D.H., L.-S. Bai, and G.G. Bjarnason, 2005: High resolution regional climate simulations over Iceland using Polar MM5: 1991- 2000.*Mon. Wea. Rev.*,**133**, 3527-3547.

——, ——, and L.-S. Bai, 2009a: Development and testing of Polar WRF: 2. Arctic Ocean. *J. Geophys. Res.*,**114**, D08122, doi:10.1029/2008 JD010300.

——, B. Kuo, M.C. Serreze, J.E. Walsh, F. Chen, K. Hines, L.-S Bai, S. H. Wang, A. Slater, W.L. Chapman, H. Huang, M. Barlage, T.K. Wee, Z. Liu, H. Lin, S. Rizvi, W. Wang, P.R. Berger, and L. Li, 2009b: Arctic System Reanalysis: progress and plans. *Extended Abstracts, 10th Conf. on Polar Meteorology and Oceanography*, Madison, WS, Amer. Meteor. Soc., in press.

Comiso, J. 1999, updated 2008: *Bootstrap sea ice concentrations from NIMBUS-7 SMMR and DMSP SSM/I*, [November 30, 2007-January 1, 2008]. Boulder, Colorado USA: National Snow and Ice Data Center. Digital media.

——, D.J. Cavalieri, and T. Markus, 2003: Sea ice concentration, ice temperature, and snow depth using AMSR-E Data. *IEEE Transactions on Geoscience and Remote Sensing*, **41**, 243-252.

Dudhia, J., 1993: A nonhydrostatic version of the Penn State-NCAR mesoscale model: Validations tests and simulation of Atlantic cyclone and cold front. *Mon. Wea. Rev.*, **121**, 1493-1513.

Durre, I., and X. Yin, 2008: Enhanced radiosonde data for studies of vertical structure. *Bull. Am. Meteorol. Soc.*, **89,** 1257-1262.

Gemmill, W., B. Katz, and X. Li, 2007: Daily Real-Time Global Sea Surface Temperature - High Resolution Analysis at NOAA/NCEP. NOAA / NWS / NCEP / MMAB Office Note Nr. **260**, 39 pp (10.0 Mb pdf file)

Grell, G.A., and D. Devenyi, 2002: A generalized approach to parameterizing convection combining ensemble and data assimilation techniques. *Geophys. Res. Lett.*, **29**, doi:10.1029/2002GL015311.

Hines, K.M., and D.H. Bromwich, 2008: Development and Testing of Polar WRF Part I: Greenland Ice Sheet Meteorology. *Mon. Wea. Rev.*, **136**, 1971-1989, doi:10.1175/2007MWR2112.1.

——, ——, M. Barlage, and A. Slater, 2009: Arctic land simulations with Polar WRF. *Extended Abstracts, 10th Conf. on Polar Meteorology and Oceanography*, Madison, WS, Amer. Meteor. Soc., in press.

Kain, J.S., 2004: The Kain-Fritsch convective parameterization: An update. *J. Appl. Meteor.*, **43**, 170-181.

Kerr, R., 2009: Arctic summer sea ice could vanish soon but not suddenly. *Science*, **23**, 1655. Accessed on April 27, 2009. [Accessed online at www.sciencemag.org]

Lindsay, R., and J. Zhang, 2006: Assimilation of ice concentration in an ice-ocean model. *J. Atmos. and Ocean. Tech.*, **23**, 742-749.

——, ——, A. Schweiger, M. Steel, and H. Stern, 2009: Arctic sea ice retreat in 2007 follows thinning trend. *J. Clim.*, **22**, 165-176.

NSIDC, cited 2007: Arctic sea ice shatters all previous record lows. Accessed April 24, 2009. [Available online at http://nsidc.org/news/press/2007_seaiceminimum/20071001_pressrelease.html]

Perovich, D.K., E.L. Andreas, J.A. Curry, H. Eiken, C.W. Fairall, T.C. Grenfell, P.S. Guest, J. Intrieri, D. Kadko, R.W. Lindsay, M.G. McPhee, J. Morison, R.E. Moritz, C.A. Paulson, W.S. Pegau, P.O.G. Persson, R. Pinkel, J.A. Richter-Menge, T. Stanton, H. Stern, M. Sturm, W.B. Tucker III, and T. Uttal, 1999: Year on ice gives climate insights, *Eos Trans. AGU*, **80(41)**, 481, 485-486.

——, S.V. Nghiem, T. Markus, and A. Schweiger, 2007: Seasonal evolution and interannual variability of the local solar energy absorbed by the Arctic sea ice-ocean system, *J. Geophys. Res.*, **112**, C03005, doi:10.1029/2006JC003558.

Powell, D.C., T. Markus, and A. Stössel, 2005: Effects of snow depth forcing on Southern Ocean sea ice simulations. *J. Geophys. Res.*, **110**, C06001, doi:10.1029/2003JC002212.

Uttal, T., J.A. Curry, M.G. McPhee, D.K. Perovich, R.E. Moritz, J.A. Maslanik, P.S. Guest, H.L. Stern, J.A. Moore, R. Turenne, A. Heiberg, M.C. Serreze, D.P. Wylie, P.O.G. Persson, C.A. Paulson, C. Halle, J.H. Morison, P.A. Wheeler, A. Makshtas, H. Welch, M.D. Shupe, J.M. Intrieri, K. Stamnes, R.W. Lindsay, R. Pinkel, W.S. Pegau, T.P. Stanton, and T.C. Grenfell, 2002: Surface Heat Budget of the Arctic Ocean, *Bull. Am. Meteorol. Soc.*,**83**, 255-275.